J. Membrane Biol. 137, 109–118 (1994)

The Journal of
Membrane
Biology

Maxi K^+ Channels from the Apical Membranes of Rabbit Oviduct Epithelial Cells

A.F. James*, Y. Okada**

Department of Physiology, Faculty of Medicine, Kyoto University, Yoshida, Sakyo-ku, Kyoto 606-01, Japan

Received: 26 March 1993/Revised: 31 August 1993

Abstract. Large conductance (approximately 210 pS), K^+-selective channels were identified in excised, inside-out patches obtained from the apical membranes of both ciliated and nonciliated epithelial cells grown as monolayers from the primary culture of rabbit oviduct. The open probability of channels showing stable gating was increased at positive membrane potentials and was sensitive to the concentration of free calcium ions at the cytosolic surface of the patch ($[Ca^{2+}]_i$). In these respects, the channel resembled "maxi K^+ channels" found in a number of other cell types. The distributions of dwelltimes in the open state were most consistently described by two exponential components. Four exponential components were fitted to the distributions of dwelltimes in the closed state. Depolarizations and $[Ca^{2+}]_i$ increases had similar effects on the distribution of open dwelltimes, causing increases in the two open time constants (τ_{o1} and τ_{o2}) and the fraction of events accounted for by the longer component of the distribution. In contrast, calcium ions and voltage had distinct effects on the distribution of closed dwelltimes. While the three shorter closed time constants (τ_{c1}, τ_{c2} and τ_{c3}) were reduced by depolarizing membrane potentials, increases in $[Ca^{2+}]_i$ caused decreases in the longer time constants (τ_{c3} and τ_{c4}). It is concluded that oviduct large conductance Ca^{2+}-activated K^+ channels can enter at least two major open states and four closed states.

Key words: Oviduct — Epithelium — Apical membrane — Maxi K^+ channels

Introduction

The epithelium of the rabbit oviduct is responsible for the oestrogen-dependent secretion of an alkaline fluid which forms the environment for gamete transport and fertilization of the oocyte (Leese, 1988). Little is known of the mechanisms by which this fluid is secreted; however, the epithelium of the rabbit oviduct is electrically "leaky" and actively transports Cl^- ions from the serosa to the lumen when mounted in Ussing chambers (Brunton & Brinster, 1971). Furthermore, both fluid secretion and Cl^- ion transport were inhibited by cyclic AMP and inhibitors of Cl^- transport in the *in situ,* vascularly perfused oviduct (Gott et al., 1988). This would suggest that the secretion of fluid by the oviduct, similar to many other epithelial and exocrine tissues, is coupled to transepithelial Cl^- transport.

The function of epithelia is dependent upon the activity of ion channels in both the apical and basolateral membranes. The stimulation of Cl^- secretion is associated with the coordinated activation of K^+ channels in the basolateral membrane and Cl^- channels in the apical membrane of exocrine tissues and airway epithelia (Petersen & Gallacher, 1988; McCann & Welsh, 1990). A role in Cl^- secretion has also been suggested recently for additional K^+ channels in the apical

* *Present address:* Bio-organics Department, International Research Laboratories, Ciba-Geigy (Japan) Ltd., 10-66 Miyuki-cho, Takarazuka 665, Japan

** *Present address:* Department of Cellular and Molecular Physiology, National Institute for Physiological Sciences, Okazaki 444, Japan

Correspondence to: Y. Okada

membrane (Cook & Young, 1989; Wehner, Winterhager & Petersen, 1989). Certainly, a significant K^+ permeability is present in the apical membrane of other leaky epithelia associated with fluid secretion (Zeuthen et al., 1987). Moreover, the fluid secreted by the oviduct contains a K^+ concentration above that of the plasma (Leese, 1988), suggesting that there is efflux of K^+ from the cell across the apical membrane during secretion.

To investigate the K^+ channels present in the apical membrane of rabbit oviduct epithelial cells, we made unitary current recordings from excised inside-out patches obtained from monolayers of cells in primary culture. We report the presence of a large conductance K^+ channel with gating properties qualitatively similar to those found in other leaky epithelia. The present work represents the first full report of recordings from ion channels in oviduct epithelial cell membranes. Some of the data have been presented previously in abstract form (James & Okada, 1991).

Materials and Methods

Culture Preparation

Monolayers of oviduct epithelial cells were grown in primary culture from explants of oviduct tissue obtained from 2.5–3.0 kg virgin female Japanese white rabbits. Animals were anesthetized with 2 ml of a 50% dilution (in HEPES-buffered saline) of sodium pentobarbital (50 mg/ml NEMBUTAL, Dainabot, Osaka) by injection into the lateral ear vein and were subsequently killed by an overdose of the same anesthetic. The culture techniques were essentially the same as those which have been used previously in a study of the rat gastric fundus (Okada & Ueda, 1984). After excision of the oviducts into ice-cold phosphate-buffered saline, the fimbriae were minced using fine-forceps and spread on sterile plastic petri dishes. They were cultured in 5 ml of Medium 199 supplemented with 20% newborn calf serum in a humidified, 5% CO_2 atmosphere at 37°C and were used for experiments between two and six days after culture. The culture medium was changed on the third day after culture. It was found that the seal resistance of excised inside-out patches from the apical membrane was improved if the culture medium was also changed approximately 12 hr prior to experiments.

Culture Media

All solutions for primary culture of oviduct epithelial cells were made using double-distilled water filtered through a micropore filter. Phosphate-buffered saline (pH 7.2) contained (mM) NaCl (127.02), KCl (2.70), Na_2HPO_4 (8.02), KH_2PO_4 (1.47), mannitol (20.00), $MgCl_2$ (0.50) and $CaCl_2$ (0.90). Culture medium was made up of Medium 199 (M199, 9.9 g/liter, Nissui Pharmaceutical, Tokyo), $NaHCO_3$ (1.0 g/liter), newborn calf serum (20%, Flow Laboratories, McLean, VA), streptomycin (0.1 g/liter) and penicillin G (100 000 U/liter). The antibiotics were supplied by Meiji Seika, Tokyo.

Experimental Solutions

Prior to perfusion of experimental solutions, cultures were bathed in HEPES-buffered saline containing (mM) NaCl (137.5), KCl (4.2), Na-HEPES (6.0), HEPES (8.0), mannitol (20.0), $MgCl_2$ (0.5) and $CaCl_2$ (0.9). Better seals were obtained if the cultures were washed several times with this saline before experiments.

Patch pipettes were filled with the HEPES-buffered saline for cell-attached experiments and KCl-rich (pH 7.4) solution containing (mM) KCl (147.00), $CaCl_2$ (1.00), $MgCl_2$ (1.00), ethyleneglycol-bis-(β-aminoethylether)-*N,N,N′,N′*–tetraacetic acid (EGTA, 1.00), Na-HEPES (10.00) and HEPES (10.00) for experiments in the excised, inside-out configuration. Low KCl solution (pH 7.4) contained (mM) Na-gluconate (116.10), KCl (30.90), $CaSO_4$ (1.00), $MgSO_4$ (1.60), EGTA (1.00), Na-HEPES (10.00) and HEPES (10.00). Experimental KCl-rich solutions from the perfusion pipette were identical to those used to fill the patch pipette except for their calcium content. The free calcium ion concentrations of these solutions were calculated using a BASIC routine from the stability constants of EGTA for Ca^{2+}, Mg^{2+}, and H^+ (Martell & Smith, 1974) by taking the purity of EGTA and the activity of H^+ into consideration (Oiki & Okada, 1987). The pH of experimental solutions was adjusted using KOH. Unless otherwise stated, all solutes were supplied by Nacalai Tesque (Kyoto).

Patch-Clamp Recordings

Patch pipettes were pulled from Pyrex glass capillaries (Summit Medical, Tokyo) using a Narishige PP-83 pipette puller and had a tip resistance of approximately 5 MΩ. Recordings were started immediately after giga-seal formation in cell-attached experiments and after lifting the patch pipette upwards, away from the cell, in experiments using the excised, inside-out configuration of the patch-clamp technique (Hamill et al., 1981). Because it was possible to form membrane vesicles in the pipette tip after excision from the cell membrane, excised patches in which no channel activity was observed were routinely passed through the air-solution interface. In some cases, this action resulted in the recording of single channel events from a patch which had previously been quiescent. Currents were amplified using an EPC-7 patch-clamp amplifier (List Medical, Germany) and recorded through a pulse-code modulation system (Sony PCM501ES) to a VHS recorder. Prior to sampling by computer, the records were filtered using an 8-pole Bessel filter with a −3 dB cut-off frequency of 2 kHz (NF Instruments FV 664). Recorded currents were sampled at intervals of 100 μsec (10 kHz) and pulse widths of 200 μsec resulted in threshold crossings. Experimental solutions were perfused through a perfusion pipette at a rate of approximately 1.9 ml/min. The patch pipette and perfusion pipette were carefully manipulated so that the tip of the patch pipette could be seen immediately beneath the relatively wider tip of the perfusion pipette under the phase-contrast optics of the light microscope. In this way, we were confident of the solution change at the tip of the patch pipette.

Data Analysis

Data were collected from patches which had stable and significant channel activity. If the channel exhibited exceptionally long closed periods (several tens of seconds) for unknown reasons, the data were discarded. Analyses were performed on IBM AT compatible computers (ALR 386SX and Sony PCX-300) using pCLAMP software (Version 5.1, Axon Instruments) or BASIC routines we developed ourselves. Idealized records were formed using a 50% threshold technique. The open probability (P_o) was calculated as the propor-

tion of time spent in the open state. The single channel P_o's from patches showing more than one channel were estimated by Newton's method assuming a binomial distribution of open probability. The number of channels present in a patch was assumed to be the maximum number of conductance levels observed under conditions associated with high P_o. The usefulness of logarithmic bins in considering the entire range of the open and closed dwelltime distributions has been demonstrated by Sigworth and Sine (1987). The dwelltime distributions were therefore formed in logarithmic bins at 8 bins/decade. To avoid the distortion of the distributions of dwelltimes caused by the limited bandwidth of our equipment, events of less than 0.3 msec in duration were ignored (Colquhoun & Sigworth, 1983). Single- or multi-exponential functions (Sigworth & Sine, 1987) were fitted to the distributions of dwelltimes. The smallest bin (0.24–0.32 msec) was not considered in fitting the distributions. Each exponential component of the fitted functions was represented by two parameters, a time constant (τ) and a weighting, representing the number of events accounted for by that component (Sigworth & Sine, 1987). No corrections were made for missed and eliminated events. The τ values reported in this paper are therefore overestimates of the τ of the hypothetical true dwelltime distributions that would be recorded by a machine of infinite bandwidth in the absence of noise (Colquhoun & Sigworth, 1983). The fraction of events (F) accounted for by each exponential component of the distributions reported in this paper were calculated from the fitted weightings. The functions were fitted by minimization of chi-squared (Schreiner et al., 1985; Press et al. 1989). Fitting was carried out from several sets of starting parameters to ensure that the best fit was obtained. Fits were accepted when addition of an extra exponential component did not lead to a significant improvement in the fit. In cases where the number of exponential components required to fit the data obtained under different conditions (membrane potential and free calcium concentration) from the same patch were not the same, the minimum number of components required to consistently describe all the data were used. The fits reported in this paper were achieved using the Marquardt algorithm supplied with pCLAMP software.

All data presented in the text are given as a mean ± SEM and statistical significance was assessed by Student's t-test at the $P < 0.05$ level.

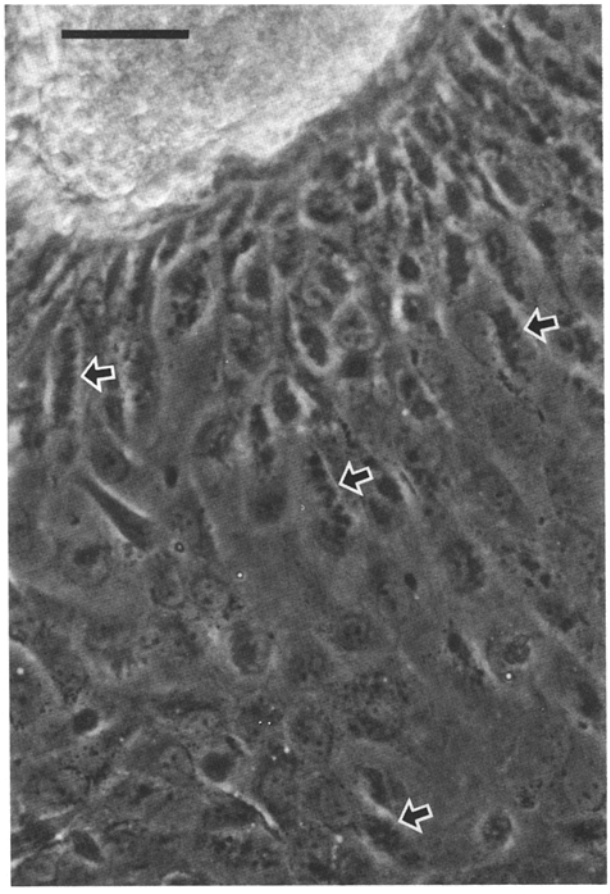

Fig. 1. A phase-contrast micrograph of a monolayer of rabbit epithelial cells in primary culture. Before the photograph was taken, cells were fixed using a 0.1% formaldehyde solution to stop the beating of cilia (arrows). The lighter mass (upper left) represents an explant of the tissue from which the culture was grown. Bar = 50 μm.

Results

Morphological Characteristics of Cultured Epithelial Cells

Two hundred and ninety two cultures of epithelial cells were obtained from explants of fimbrial tissue obtained from 42 rabbits. Epithelioid cells started to spread radially from the explants of oviduct tissue on the second day of culture, forming a developing island of cells in a monolayer by the third day. These islands of monolayers contained ciliated cells (38.1 ± 3.5%, $n = 13$; Fig. 1, arrows), indicating that the cultures were comprised of epithelial cells. Some of the explanted tissues, which failed to adhere to the culture dish, formed floating globular fragments that were often seen to be rotating due to ciliary movement. The monolayer island became confluent after six days in culture, being surrounded by a monolayer of fibroblastic cells.

Transmission electron micrographs (*data not shown*) revealed the presence of cilia and microvilli on the uppermost surface, tight junctions at the upper end of the intercellular space and desmosomes in the lower region. These findings confirm that the monolayers were formed by epithelial cells maintaining their morphological polarity with the apical surface uppermost. Only monolayers in which ciliated cells were present were used in this study. Patches were only obtained from the center of monolayer islands near to the tissue explant.

Large Conductance K^+ Channels in the Apical Membrane

In a group of 11 cell-attached patches of the membrane of the upper surface of these monolayers, with the pipette filled with the extracellular HEPES-buffered bathing solution, no outward currents could be seen at a pipette potential of −30 mV. However, after expo-

sure of the cells to a combination of 3 μM of the calcium ionophore, ionomycin and 10 μM of the intracellular calcium-release channel activator, ryanodine, outward unitary currents of approximately 8 pA were briefly activated in two of the patches. After excision and exposure of the cytosolic surface of the patches to a high KCl solution, outward currents were observed at a membrane potential of 0 mV, suggesting that these were K^+-selective channels. The single channel conductance estimated by linear regression was 203 pS.

Excised, inside-out patches (n = 859) were obtained from the upper surface of the monolayers with the pipette filled with the high KCl solution. Several different types of current were recorded but the most common (n = 162) were large conductance K^+ currents which were identified on the basis of their current-voltage relation with the HEPES-buffered saline bathing the inner surface of the patch. Channel activity was occasionally recorded from patches which had previously been quiescent after passing the pipette through the air/solution interface. The voltage dependence and conductance properties of such channels were the same as those obtained without passage of the pipette tip through the air-solution interface.

These K^+ currents were obtained from ciliated and nonciliated cells. In a preliminary study of 21 channel-containing patches obtained from ciliated and nonciliated cells alternatively, channels were found in 13 patches from ciliated cells and 8 patches from nonciliated cells. The mean number of channels in 66 patches exposed to KCl solutions at 10 μM $[Ca^{2+}]_i$ was 1.39 ± 0.09. Forty eight patches contained 1 channel, 12 contained 2 channels, 5 contained 3 channels and one contained 5 channels.

Examination of the current traces from a single patch (Fig. 2*A*) demonstrates that the channel showed clear open and shut states. However, subconductance states in which current flow was approximately 50% of the full conductance were occasionally (0.1 to 1% of sojourns) observed (Fig. 2*B*). Since sojourns in this subconductance state were very rare, they were set to zero-conductance level in analyses of the P_o and dwelltimes of the channel. The pooled data from 11 such patches, which were superfused with both low KCl and KCl-rich solutions, are shown in Fig. 2*C*. The direction of current flow through these channels reversed at, or very near, +40 mV in low KCl and 0 mV in KCl-rich solutions—values equivalent to the equilibrium potential for K^+ ions, suggesting that this channel was strongly K^+ selective. The mean single channel conductance under symmetrical K^+ conditions was 213.10 ± 5.30 pS (n = 11). Examination of the current traces in Fig. 2*A* shows that the channel spent more time in the open state at positive membrane potentials. The dependency of channel P_o on the membrane potential of this patch is shown in Fig. 2*D*.

Current traces from another experiment in which the cytoplasmic surface of a patch containing a single channel was held at +40 mV and superfused with 147 mM KCl solutions of various free calcium concentrations (Fig. 3*A*) demonstrate that the probability of the channel being in the open state was dependent upon the concentration of free calcium ions at the cytosolic surface ($[Ca^{2+}]_i$) of the patch. The dependence of the channel P_o upon $[Ca^{2+}]_i$ at four different membrane potentials for this patch is shown in Fig. 3*B*. The channel open probability was increased by both increases in $[Ca^{2+}]_i$ and membrane depolarizations. Since the maximal P_o (0.77) was less than 1.00 at 100 μM $[Ca^{2+}]_i$ and +80 mV, the gating kinetics of the channel could not be considered in terms of a simple Hill-type equilibrium between the channel and Ca^{2+} ions. However, log-log plots of P_o against $[Ca^{2+}]_i$ gave maximum slopes of approximately 2, suggesting that the binding of at least two calcium ions was involved in channel gating.

The channels showed activity distributed around a mean P_o of 0.238 ± 0.018 at −40 mV which increased to 0.651 ± 0.053 at +40 mV (n = 18; $P < 0.001$) in solutions containing 10 μM $[Ca^{2+}]_i$. The mean effective gating charge obtained by fitting the data to a Boltzmann distribution was 0.723 ± 0.083 (n = 3). In a separate set of experiments conducted at +40 mV, the mean P_o increased from 0.202 ± 0.036 at 1 μM $[Ca^{2+}]_i$ to 0.643 ± 0.050 at 10 μM $[Ca^{2+}]_i$ (n = 3; $P < 0.01$). Only 1 out of 24 patches exposed to KCl solutions at 0.1 μM $[Ca^{2+}]_i$ showed significant open probability (0.43) at +40 mV. All these channels were open immediately after excision when exposed to HEPES-buffered saline containing 0.9 mM $[Ca^{2+}]_i$.

Gating Kinetics of the Large Conductance K^+ Channel

The gating of the large conductance K^+ channel was considered further in terms of the distributions of dwell-times in the open and closed states of the patches shown in Figs. 2 and 3. The dwelltime distributions for the patch shown in Fig. 2*A* at +40 and −40 mV are shown in Fig. 4. At −40 mV, channel openings of up to about 50 msec were observed with a single peak to the distribution at around 3 msec. Although only one peak was discernible, two exponential components, with time constants (τ) of 0.652 and 3.34 msec, were required to adequately fit the distribution (Fig. 4*Aa*). The long component accounted for 76.2% of open dwelltimes. Depolarizing the membrane to +40 mV shifted the distribution to the right so that open dwelltimes of up to 100 msec were observed with a broad peak around 15 msec (Fig. 4*Ab*). Both components of the distribution were shifted to the right, so that the short component had a τ of 1.77 msec while the long component had a τ of

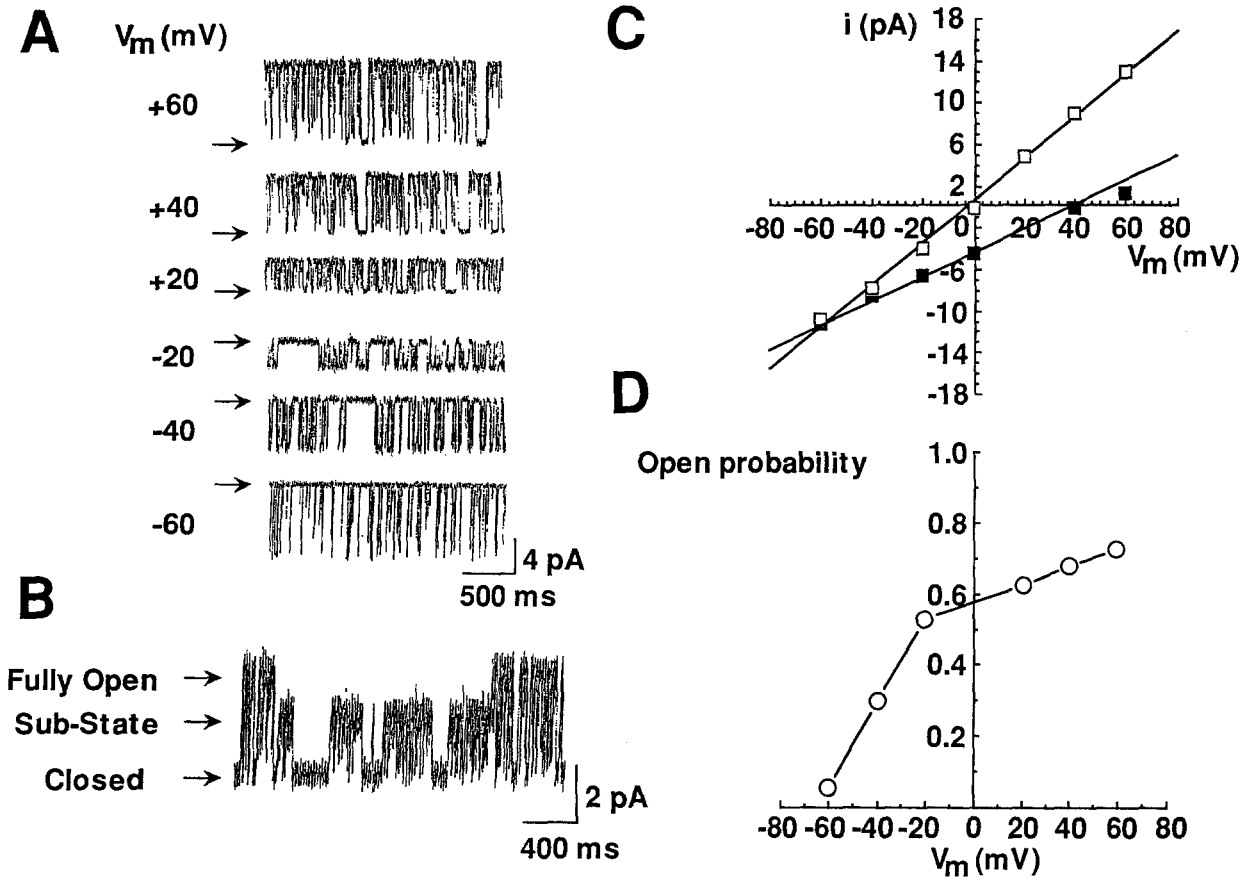

Fig. 2. Voltage dependence of maxi K^+ channel activity. (*A*) Examples of recordings of unitary current from a maxi K^+ channel. The patch was perfused with a KCl solution at a pH_i of 7.4 and a $[Ca^{2+}]_i$ of 10 μM. Membrane potentials (V_m) were as indicated. The arrows indicate the closed state. This patch contained only one channel. (*B*) Recordings from the same patch at a membrane potential of +20 mV. These show the existence of a subconductance state. (*C*) The current-voltage relation of mean unitary currents (*i*) through 11 channels superfused with both KCl (open squares) and low KCl (filled squares) solutions at the cytosolic surface of the membrane. The equilibrium potential for K^+ ions across the patch membrane when the patch was perfused with low KCl solutions was +40 mV. That for Cl^- ions was −40 mV. Each data point is shown as the mean ± SEM. The standard error bars were smaller than the symbols used. (*D*) The voltage dependency of the P_o for the channel shown in *A*.

11.7 msec. However, the fraction of events accounted for by the short component (F_{o1}) decreased at +40 mV. By contrast to the distribution of open dwelltimes, there was no single discernible peak to the closed dwelltime distribution at −40 mV, event as long as 300 msec being observed (Fig. 4*Ba*). Moreover, unlike the open dwelltime distribution, changing the membrane potential to +40 mV had very little influence on the range of times over which closures were distributed (Fig. 4*Bb*). Four exponential components were fitted to the distribution of closed dwelltimes. The predominant effects of membrane depolarization were to shorten τ_{c3} and reduce the fraction of events accounted for by this component of the distribution (F_{c3}), and to increase concomitantly the fraction of events accounted for by the shortest component of the distribution (F_{c1}) (Fig. 4*B*). Thus, at +40 mV, two major peaks to the distribution of closed dwelltimes could be distinguished.

The effects of membrane potential between −60 and +60 mV are also shown in Fig. 4 in terms of the time constants (τ) and fraction of events (*F*) of the dwelltime distributions. Depolarizations resulted in increases in both time constants (τ_{o1} and τ_{o2}) of the open dwelltime distribution (Fig. 4*Ac*) and in the fraction of events accounted for by the longer component of the distribution (F_{o2}; Fig. 4*Ad*). Depolarizing the membrane potential shortened τ_{c1}, τ_{c2} and τ_{c3} of the closed dwelltime distribution (Fig. 4*Bc*). However, the longest component (τ_{c4}) did not change significantly over the range from −60 to +60 mV (Fig. 4*Bc*), reflecting the lack of effect of membrane potential on the maximum duration of closures. Depolarizing the membrane led to a de-

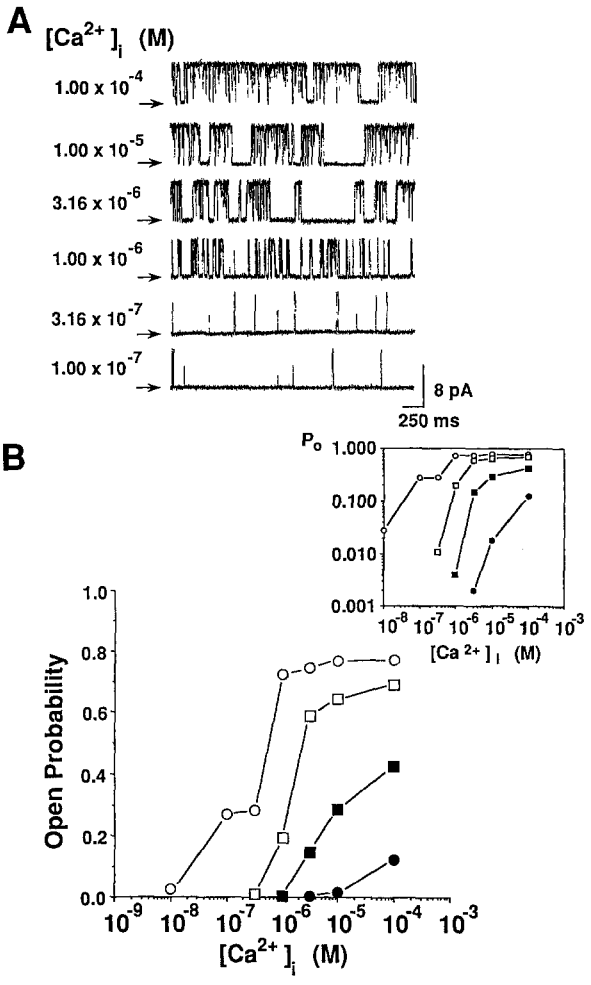

Fig. 3. Calcium dependence of maxi K^+ channel activity. (*A*) Current traces of a patch held at +40 mV and superfused with 147 mM KCl solutions of the indicated free calcium concentration. (*B*) The relationship between free calcium concentration and channel P_o at various membrane potentials for the channel shown in *A*. Open circles, +80 mV; open squares, +40 mV; filled squares, −40 mV; and filled circles, −80 mV. The mean maximum slope of the log-log plots of the data shown here (inset) was 2.13 ± 0.47 (n = 4).

crease in F_{c3} and a concomitant increase in F_{c1} (Fig. 4*Bd*). Similar voltage dependency of the τ and F of the dwelltime distributions was observed in paired experiments from three patches. The mean τ_{o1}, τ_{o2}, F_{o1}, and F_{o2} of the open dwelltime distributions were 0.761 ± 0.061 msec, 3.81 ± 0.973 msec, 0.255 ± 0.064 and 0.745 ± 0.064 at −40 mV, and 1.77 ± 1.77 msec, 15.7 ± 3.71 msec, 0.020 ± 0.020 and 0.980 ± 0.020 at +40 mV, respectively (n = 3). The mean τ_{c1}, τ_{c2}, τ_{c3}, τ_{c4}, F_{c1}, F_{c2}, F_{c3} and F_{c4} of the closed dwelltime distribution were 0.347 ± 0.012 msec, 1.42 ± 0.422 msec, 15.64 ± 6.70 msec, 78.1 ± 40.6 msec, 0.357 ± 0.052, 0.263 ± 0.044, 0.232 ± 0.063 and 0.148 ± 0.077 at −40 mV, and 0.296 ± 0.029 msec, 1.02 ± 0.261 msec, 7.72 ± 3.29 msec, 81.9 ± 19.7 msec, 0.702 ± 0.027, 0.190 ± 0.037, 0.043 ± 0.011 and 0.066 ± 0.017 at +40 mV, respectively.

The distributions of open and closed dwelltimes for the patch shown in Fig. 3*A* at +40 mV with 1 and 10 μM Ca^{2+} are shown in Fig: 5. At 1 μM $[Ca^{2+}]_i$, open events of up to about 75 msec were recorded, with a single peak to the distribution at around 7 msec (Fig. 5*Aa*). The open dwelltime distribution was fitted by two exponential components at this $[Ca^{2+}]_i$. The tenfold increase in $[Ca^{2+}]_i$ caused a rightward-shift in the distribution so that openings of up to 178 msec were observed, distributed around a peak of approximately 13 msec (Fig. 5*Ab*). Both time constants of the open dwelltime distribution were dependent on $[Ca^{2+}]_i$ between 0.316 and 3.16 μM (Fig. 5*Ac*). However, at higher Ca^{2+} concentrations (10 and 100 μM) the distribution of open dwelltimes was well fitted by a single exponential component because the fraction of events accounted for by the shorter component (F_{o1}) decreased as the membrane potential became more positive (Fig. 5*Ad*). At 10 and 100 μM, F_{o1} was so small that it was difficult to distinguish the shorter component from the longer exponential component. Two major peaks to the distribution of closed dwelltimes could be distinguished at 1 μM with events of up to 1,300 msec being recorded (Fig. 5*Ba*). Increasing $[Ca^{2+}]_i$ caused a slight leftward-shift in the distribution, so that the maximum duration of events was approximately 750 msec (Fig. 5*Bb*). This was reflected in Ca^{2+}-dependent decreases of the time constants of the longer components (τ_{c3} and τ_{c4}) of the distribution (Fig. 5*Bc*). Unlike the effect of depolarizing the cell membrane, increasing $[Ca^{2+}]_i$ did not significantly reduce the time constants of the shorter components (τ_{c1} and τ_{c2}). F_{c1} increased with increasing $[Ca^{2+}]_i$, consistent with the effect of membrane depolarization (Fig. 5*Bb* and *Bd*). However, in contrast to the effect of membrane potential, this increase in F_{c1} was concomitant with a decrease in F_{c4}, with apparently little effect of $[Ca^{2+}]_i$ on F_{c3}.

Similar effects of $[Ca^{2+}]_i$ were observed on the τ and F of the dwelltime distributions recorded in paired experiments from three patches at +40 mV. The mean τ_{o1}, τ_{o2}, F_{o1} and F_{o2} of the open dwelltime distribution were, respectively, 0.651 ± 0.194 msec, 6.02 ± 0.161 msec, 0.120 ± 0.050 and 0.880 ± 0.050 at 1 μM $[Ca^{2+}]_i$. At 10 μM $[Ca^{2+}]_i$, the mean τ_{o2} was 12.2 ± 1.3 msec. The mean τ_{c1}, τ_{c2}, τ_{c3}, τ_{c4}, F_{c1}, F_{c2}, F_{c3} and F_{c4} of the closed dwelltime distribution were 0.411 ± 0.086 msec, 165 ± 0.38 msec, 56.9 ± 10.2 msec, 167.8 ± 10.1 msec, 0.477 ± 0.111, 0.218 ± 0.054, 0.114 ± 0.020 and 0.039 ± 0.01 at 1 μM $[Ca^{2+}]_i$, and 0.287 ± 0.058 msec, 0.991 ± 0.446 msec, 9.84 ± 9.01 msec, 83.8 ± 21.4 msec, 0.721 ± 0.047, 0.169 ± 0.025, 0.043 ± 0.027 and 0.068 ± 0.044 at 10 μM $[Ca^{2+}]_i$, respectively.

The effect of increasing $[Ca^{2+}]_i$ on the distribution

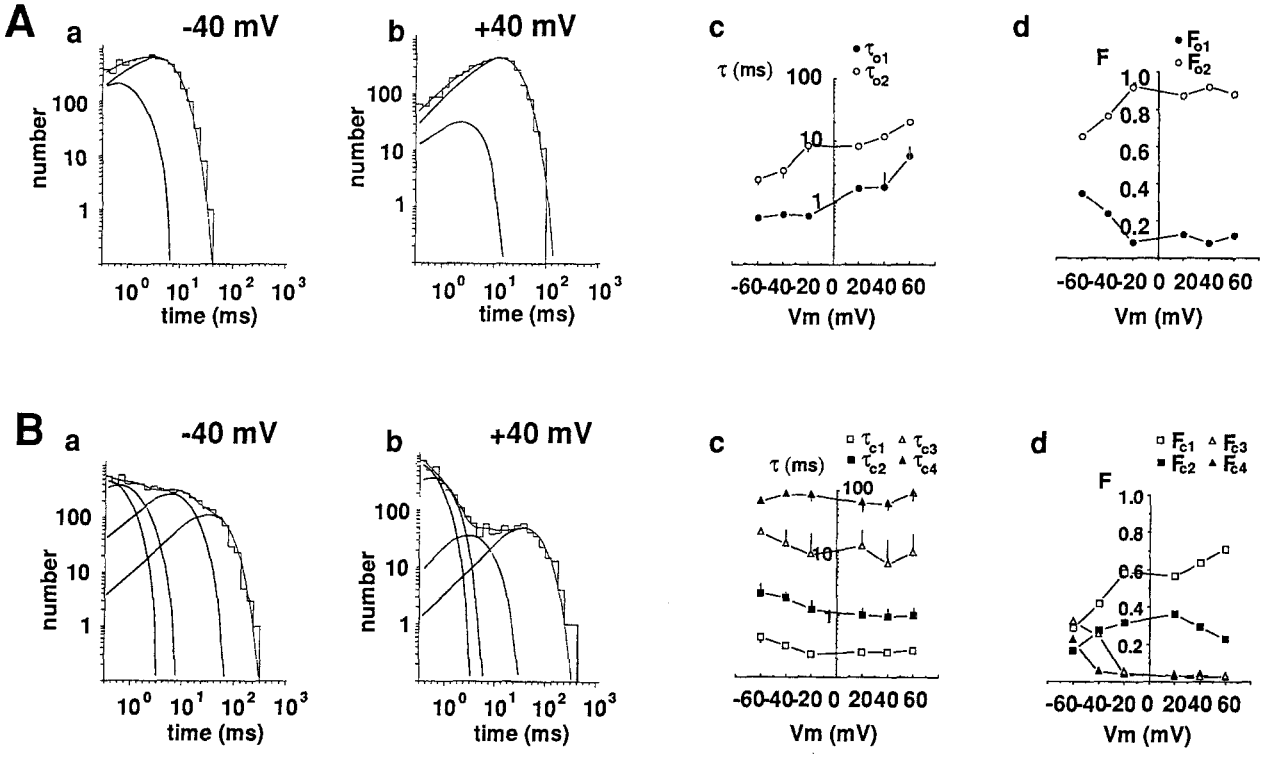

Fig. 4. Dependency of channel gating on membrane potential (V_m). Same channel as Fig. 2*A*. Events were binned from 60 sec recordings of channel activity. (*A*) The distribution of open dwelltimes (*a,b*) formed in logarithmic bins at 8 bins/decade, the time constants (*c*) and the fractions of events (*d*). (*a*) −40 mV. 6,668 events. τ_{o1} = 0.652 msec, F_{o1} = 0.238, τ_{o2} = 3.34 msec, F_{o2} = 0.762. (*b*) +40 mV. 4,293 events. τ_{o1} = 1.77 msec, F_{o1} = 0.080, τ_{o2} = 11.7 msec and F_{o2} = 0.920. (*c*) The open time constants, τ_{o1} (filled circles) and τ_{o2} (open circles) between −60 and +60 mV. (*d*) The fractions of events F_{o1} (filled circles) and F_{o2} (open circles) between −60 and +60 mV. (*B*) The distribution of closed dwelltimes (*a,b*), the time constants (*c*) and the fractions of events (*d*). (*a*) −40 mV. 6,669 events. τ_{c1} = 0.326 msec, F_{c1} = 0.417, τ_{c2} = 1.87 msec, F_{c2} = 0.273, τ_{c3} = 14.2 msec, F_{c3} = 0.255, τ_{c4} = 89 msec and F_{c4} = 0.054. (*b*) +40 mV. 4,293 events. τ_{c1} = 0.252 msec, F_{c1} = 0.635, τ_{c2} = 0.926 msec, F_{c2} = 0.294, τ_{c3} = 6.65 msec, F_{c3} = 0.028, τ_{c4} = 61.5 msec and F_{c4} = 0.043. (*c*) The closed time constants, τ_{c1} (open squares), τ_{c2} (filled squares), τ_{c3} (open triangles) and τ_{c4} (filled triangles) between −60 and +60 mV. (*d*) The fractions of events, F_{c1} (open squares), F_{c2} (filled squares), F_{c3} (open triangles) and F_{c4} (filled triangles) between −60 and +60 mV. The bars represent the fitting error associated with each time constant.

of open dwelltimes was similar to that of making the membrane potential positive; both manipulations were associated with increases in τ_{o1}, τ_{o2} and F_{o2}. In contrast, while both τ_{c3} and τ_{c4} of the closed dwelltime distribution were strongly sensitive to $[Ca^{2+}]_i$, τ_{c1}, τ_{c2} and τ_{c3} showed weak voltage dependency over the physiological range of membrane potentials. Moreover, although both positive membrane potentials and increases in $[Ca^{2+}]_i$ were apparently associated with increases in F_{c1}, increasing $[Ca^{2+}]_i$ resulted in decreases in F_{c4}, which was relatively unaffected by membrane potential. Conversely, membrane depolarization decreased F_{c3}, which was relatively insensitive to $[Ca^{2+}]_i$.

Discussion

We have identified a class of large conductance K^+ channels in records of single channel currents from excised inside-out patches of cultured rabbit oviduct epithelial membranes. The conductance (approximately 210 pS), the activation of single channel currents at more positive membrane potentials (Fig. 2) and the regulation of channel gating by calcium at the intracellular surface of the membrane (Fig. 3) resemble large conductance K^+, or maxi K^+, channels found in many other cell types. Maxi K^+ channels were divided by Gray and co-authors (1990) into three groups by considering the calcium concentration and membrane potential at which the open probability was equal, or nearly equal, to 0.5. The oviduct channel was only open for a significant proportion of the time at $[Ca^{2+}]_i$ above 0.316 μM at positive membrane potentials and can therefore be assigned to a group showing low sensitivity to $[Ca^{2+}]_i$ which includes maxi K^+ channels from skeletal muscle (Moczydlowski & Latorre, 1983; McManus & Magleby, 1991), pancreatic islets (Cook, Ikeuchi & Fujimoto, 1984; Findlay, Dunne & Petersen, 1985) and

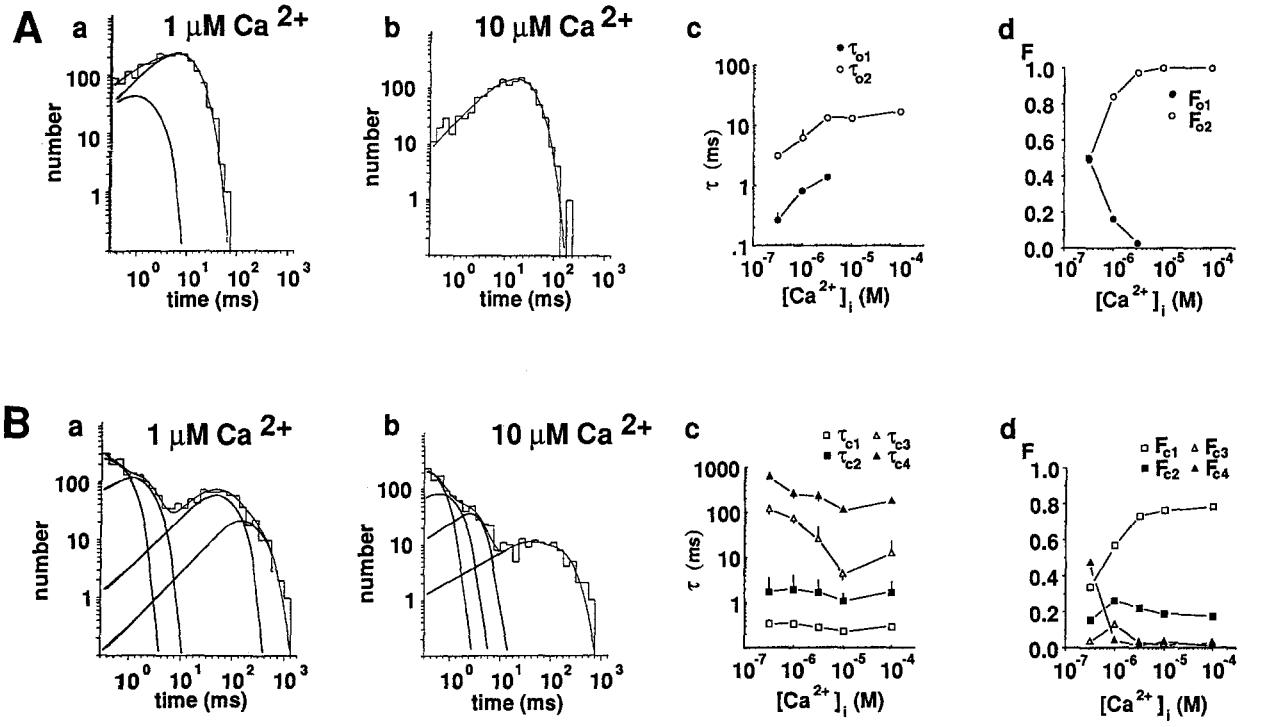

Fig. 5. Dependency of channel gating on $[Ca^{2+}]_i$. Symbols as in Fig. 4. Same channel as Fig. 3. Events were binned from 60 sec recordings of channel activity. (*A*) The distribution of open dwelltimes (*a,b*), the time constants (*c*) and the fraction of events (*d*). (*a*) 1 μM. 2,351 events. τ_{o1} = 0.807 msec, F_{o1} = 0.491, τ_{o2} = 6.15 msec, F_{o2} = 0.509. (*b*) 10 μM. 1,174 events. τ_{o2} = 13.3 msec with weighting 407.21. (*c*) The open time constants, τ_{o1} and τ_{o2}, between 0.316 and 100 μM $[Ca^{2+}]_i$. (*d*) The fractions of events, F_{o1} and F_{o2}, between 0.316 and 100 μM $[Ca^{2+}]_i$. (*B*) The distribution of closed dwelltimes (*a,b*), the time constants (*c*) and the fraction of events (*d*). (*a*) 1 μM. 2,350 events. τ_{c1} = 0.341 msec, F_{c1} = 0.337, τ_{c2} = 1.94 msec, F_{c2} = 0.154, τ_{c3} = 74.4 msec, F_{c3} = 0.037, τ_{c4} = 269 msec and F_{c4} = 0.472. (*b*) 10 μM. 1,175 events. τ_{c1} = 0.240 msec, F_{c1} = 0.759, τ_{c2} = 1.10 msec, F_{c2} = 0.188, τ_{c3} = 4.51 msec, F_{c3} = 0.021, τ_{c4} = 116 msec and F_{c4} = 0.032. (*c*) The closed time constants, τ_{c1}, τ_{c2}, τ_{c3} and τ_{c4}, between 0.316 and 100 μM $[Ca^{2+}]_i$. (*b*) The fractions of events. The bars represent the fitting error associated with each time constant.

epithelia such as the amphibian choroid plexus (Christensen & Zeuthen, 1987; Brown, Loo & Wright, 1988) and the rat pancreatic duct (Gray et al., 1990). However, the voltage dependency of the oviduct channel was considerably weaker than that of other similar maxi K^+ channels. The effective gating charge reported for the large conductance K^+ channels from rat skeletal muscle (Latorre, Vergara & Hidalgo, 1982) and amphibian choroid plexus (Christensen & Zeuthen, 1987) (z = 2) is larger than that of the oviduct channel (z = 0.7).

Since two components were required to fit the open dwelltime distribution and four exponential components were fitted to the closed dwelltime distributions (Figs. 4 and 5), at least two open states and four closed states would be necessary to describe the gating kinetics of the oviduct channel (Colquhoun & Hawkes, 1983). The open dwelltime distributions obtained from other maxi K^+ channels have been variously fitted by one (Moczydlowski & Latorre, 1983; Christensen & Zeuthen, 1987; Sheppard, Giraldez & Sepúlveda, 1988; Cornejo, Guggino & Guggino, 1989), two (Magleby & Palotta, 1983; Kume et al., 1990) and three (McManus & Magleby, 1991) exponential components. While the closed dwelltime distributions of these channels have been fitted by two (Moczydlowski & Latorre, 1983; Christensen & Zeuthen, 1987; Sheppard et al., 1988; Kume et al., 1990), three (Magleby & Palotta, 1983; Cornejo et al., 1989) and five (McManus & Magleby, 1991) exponential components. Due to differences in the sampling intervals, filtering and binning methods used in these reports, direct comparison of the dwelltime distributions of these channels with the oviduct channel is difficult (Colquhoun & Sigworth, 1983; Sigworth & Sine, 1987).

A number of investigations have been made into the Ca^{2+}- and voltage-dependent gating kinetics of maxi K^+ channels in excised, inside-out, patches which have resulted in models involving multiple open and closed states (Magleby & Palotta, 1983; Moczydlowski & Latorre, 1983; McManus & Magleby, 1991). The binding of Ca^{2+} ions to the closed and open states cause changes in the conformation of the channel, allowing the gate to,

respectively, open and close. It was not possible to explain the Ca^{2+}- and membrane potential-dependent increases of both τ_{o1} and τ_{o2} of the open dwelltime distributions of the oviduct channel with models involving only two open states. On the other hand, we have no evidence for additional open states.

The maximum slopes of log-log plots of channel P_o against Ca^{2+} concentration indicated that at least two Ca^{2+} ions were involved in the gating of the oviduct channel (Fig. 3*B*). The Ca^{2+} ion concentration at the cytosolic surface of the patch affected both time constants of the open dwelltime distribution and two time constants of the closed dwelltime distribution, suggesting that gating might be associated with the binding of up to four Ca^{2+} ions in total; two to the open and two to the closed channels. These results are broadly in line with reports on other maxi K^+ channels in which the binding of from two to four Ca^{2+} ions have been proposed (Wong, Lecar & Adler, 1982; Magleby & Palotta, 1983; Moczydlowski & Latorre, 1983; Christensen & Zeuthen, 1987; McManus & Magleby, 1991).

The maxi K^+ channels reported here were found in the apical membranes of both ciliated and nonciliated oviduct epithelial cells in primary monolayer cultures and were activated by increases in the intracellular Ca^{2+} concentration. Potassium channels have been found in the apical membranes of a number of epithelia including the amphibian gallbladder (Copello et al., 1991) and various renal epithelia (Hunter et al., 1984; Brown & Murer, 1986; Cornejo et al., 1989), where they may be involved in K^+ secretion and fluid absorption. Recently, a role in epithelial Cl^- secretion for an apical membrane K^+ conductance has also been suggested (Cook & Young, 1989). Oviduct Cl^- secretion is thought to be regulated by neurotransmitters (Leese, 1988). Brunton (1972) demonstrated that the serosa positive transepithelial potential difference and short-circuit current across the rabbit oviduct mounted in Ussing chambers were increased by the β-adrenergic agonist, isoproterenol. Furthermore pilocarpine, which inhibits the degradation of acetylcholine, has been shown to increase the formation of rabbit oviduct fluid in vivo (Bishop, 1956). The regulation of the oviduct large conductance channel by putative secretagogues is to be the subject of future investigations.

Epithelial cells exposed to hyposmotic environments respond with a regulatory volume decrease associated with an efflux of KCl (Hoffmann & Simonsen, 1989). Parallel activation of Ca^{2+}-activated K^+ and Ca^{2+}-independent Cl^- channels has been shown to be involved in regulatory volume decrease by an epithelial cell line (Hazama & Okada, 1988). Since the secretions of the oviduct are hypotonic to the plasma at oestrous, rabbit oviduct epithelial cells may well be presented with a problem in volume regulation.

The large conductance K^+ channels reported in the present study may be involved in epithelial K^+ or Cl^- secretion or in regulatory volume decrease. However, with our present knowledge we are unable to ascribe a physiological function to this channel.

A.F.J. was supported by a research fellowship from the Japan Society for the Promotion of Science and received a grant for laboratory expenses from the Ministry of Education, Science and Culture, Japan. The authors wish to thank Dr. Shigetoshi Oiki for valuable discussion of the analysis of gating kinetics and Dr. Jeman Kim (Kyoto Pharmaceutical University) for making the transmission electron micrographs.

References

Bishop, D.W. 1956. Active secretion in the rabbit oviduct. *Am. J. Physiol.* **187:**347–352

Brown, P.D., Loo, D.D.F., Wright, E.M. 1988. Ca^{2+}-activated K^+ channels in the apical membrane of *Necturus* choroid plexus. *J. Membrane Biol.* **105:**207–219

Brunton, W.J. 1972. β-adrenergic stimulation of transmembrane potential and short-circuit current of rabbit oviduct. *Nature, New Biol.* **236:**12–14

Brunton, W.J., Brinster, R.L. 1971. Active chloride transport in the isolated rabbit oviduct. *Am. J. Physiol.* **221:**658–661

Christensen, O., Zeuthen, T. 1987. Maxi K^+ channels in leaky epithelia are regulated by intracellular Ca^{2+}, pH and membrane potential. *Pfluegers Arch.* **408:**249–259

Colquhoun, D., Hawkes, A.G. 1983. The principles of the stochastic interpretation of ion-channel mechanisms. *In:* Single Channel Recording. B. Sakmann and E. Neher, editors. pp. 135–175. Plenum, New York

Colquhoun, D., Sigworth, F.J. 1983. Fitting and statistical analysis of single-channel records. *In:* Single Channel Recording. B. Sakmann and E. Neher, editors. pp. 191–263. Plenum, New York

Cook, D.L., Ikeuchi, M., Fujimoto, W.Y. 1984. Lowering of pH_i inhibits Ca^{2+}-activated K^+ channels in pancreatic β-cells. *Nature* **311:**269–271

Cook, D.I., Young, J.A. 1989. Effect of K^+ channels in the apical plasma membrane on epithelial secretion based on secondary active Cl^- transport. *J. Membrane Biol.* **110:**139–146

Copello, J., Segal, Y., Reuss, L. 1991. Cytosolic pH regulates maxi K^+ channels in *Necturus* gallbladder epithelial cells. *J. Physiol.* **434:**577–590

Cornejo, M., Guggino, S.E., Guggino, W.B. 1989. Ca^{2+}-activated K^+ channels from cultured renal medullary thick ascending limb: Effects of pH. *J. Membrane Biol.* **110:**49–55

Findlay, I., Dunne, M.J., Petersen, O.H. 1985. High-conductance K^+ channel in pancreatic islet cells can be activated and inactivated by internal calcium. *J. Membrane Biol.* **83:**169–175

Gott, A.L., Gray, S.M., James, A.F., Leese, H.J. 1988. The mechanism and control of rabbit oviduct fluid formation. *Biol. Reprod.* **39:**758–763

Gray, M.A., Greenwell, J.R., Garton, A.J., Argent, B.E. 1990. Regulation of maxi-K^+ channels on pancreatic duct cells by cyclic AMP-dependent phosphorylation. *J. Membrane Biol.* **115:**203–215

Hamill, O.P., Marty, A., Neher, E., Sakmann, B., Sigworth, F.J. 1981. Improved patch-clamp techniques for high resolution current recording from cells and cell-free patches. *Pfluegers Arch.* **398:**85–100

Hazama, A., Okada, Y. 1988. Ca^{2+} sensitivity of volume-regulatory K^+ and Cl^- channels in cultured human epithelial cells. *J. Physiol.* **402:**682–702

Hoffmann, E.K., Simonsen, L.O. 1989. Membrane mechanisms in volume and pH regulation in vertebrate cells. *Physiol. Rev.* **69:**315–382

Hunter, M., Lopes, A.G., Boulpaep, E.L., Giebisch, G.H. 1984. Single channel recordings of calcium-activated potassium channels in the apical membrane of rabbit cortical collecting tubules. *Proc. Natl. Acad. Sci. USA* **81:**4237–4239

James, A.F., Okada, Y. 1991. Membrane potential and intracellular Ca^{2+} regulate the maxi-K^+ channel from rabbit oviduct epithelial cells. *Jpn. J. Physiol.* **41(S):**S121

Kolb, H.A., Brown, C.D.A., Murer, H. 1986. Characterization of a Ca-dependent maxi K channel in the apical membrane of a cultured renal epithelium (JTC-12.P3). *J. Membrane Biol.* **92:**207–215

Kume, H., Takagi, K., Satake, T., Tokuno, H., Tomita, T. 1990. Effects of intracellular pH on calcium-activated potassium channels in rabbit tracheal smooth muscle. *J. Physiol.* **424:**445–457

Latorre, R., Vergara, C., Hidalgo, C. 1982. Reconstitution in planar lipid bilayers of a Ca^{2+}-dependent K^+ channel from transverse tubule membranes isolated from rabbit skeletal muscle. *Proc. Natl. Acad. Sci. USA* **79:**805–809

Leese, H.J. 1988. The formation and function of oviduct fluid. *J. Reprod. Fert.* **82:**843–856

Magleby, K.L., Pallotta, B.S. 1983. Calcium dependence of open and shut interval distributions from calcium-activated potassium channels in cultured rat muscle. *J. Physiol.* **344:**585–604

Martell, A.E., Smith, R.M. 1974. Critical Stability Constants. Amino Acids. Vol. 1. Plenum, New York

McCann, J.D., Welsh, M.J. 1990. Regulation of Cl^- and K^+ channels in airway epithelium. *Annu. Rev. Physiol.* **52:**115–136

McManus, O.B., Magleby, K.L. 1991. Accounting for the Ca^{2+}-dependent kinetics of single large-conductance Ca^{2+}-activated K^+ channels in rat skeletal muscle. *J. Physiol.* **443:**739–777

Moczydlowski, E., Latorre, R. 1983. Gating kinetics of Ca^{2+}-activated K^+ channels from rat muscle incorporated into planar lipid bilayers. *J. Gen. Physiol.* **82:**511–542

Oiki, S., Okada, Y. 1987. Ca-EGTA buffer in physiological solutions. *Seitai-no-Kagaku* **38:**79–83

Okada, Y., Ueda, S. 1984. Electrical membrane responses to secretagogues in parietal cells of the rat gastric mucosa in culture. *J. Physiol.* **354:**105–119

Petersen, O.H., Gallacher, D.V. 1988. Electrophysiology of pancreatic and salivary acinar cells. *Annu. Rev. Physiol.* **50:**65–80

Press, W.H., Flannery, B.P., Teukolsky, S.A., Vetterling, W.T. 1989. Numerical Recipes: The Art of Scientific Computing. Cambridge University, UK

Schreiner, W., Kramer, M., Krischer, S., Langsan, Y. 1985. Non-linear least-squares fitting. *PC Tech. J.* **May 1985:**170–189

Sheppard, D.N., Giraldez, F., Sepúlveda, F.V. 1988. Kinetics of voltage- and Ca^{2+}-activation and Ba^{2+} blockade of a large-conductance K^+ channel from *Necturus* enterocytes. *J. Membrane Biol.* **105:**65–75

Sigworth, F., Sine, S.M. 1987. Data transformations for improved display and fitting of single-channel dwelltime histograms. *Biophys. J.* **52:**1047–1054

Wehner, F., Winterhager, J.M., Petersen, K.-U. 1989. Selective blockage of cell membrane K conductance by an antisecretory agent in guinea-pig gallbladder epithelium. *Pfluegers Arch.* **414:**331–339

Wong, B.S., Lecar, H., Adler, M. 1982. Single calcium-dependent potassium channels in clonal anterior pituitary cells. *Biophys. J.* **39:**313–317

Zeuthen, T., Christensen, O., Baerentsen, J.H., la Cour, M. 1987. The mechanism of electrodiffusive K^+ transport in leaky epithelia and some of its consequences for anion transport. *Pfluegers Arch.* **408:**260–266